Degree of dynamical charge overlap in ionic crystals*

Andrew Man† and Walter E. Bron
Department of Physics, Indiana University, Bloomington, Indiana 47401
(Received 23 June 1975)

The degree of dynamical charge overlap in $SrCl_2$:Sm^{2+} relative to that in SrF_2:Sm^{2+} has been determined from vibronic and static stress data and is compared with theoretical results obtained from a classical, extended-charge shell model. The results definitely imply that there exists less charge overlap in $SrCl_2$ than in SrF_2. An analysis based on the extended-charge shell model indicates that the major source of this result is the high electronic polarizability of the Cl^- ion compared to the F^- ion. Apparently, the electronic charge distribution of the Cl^- ion distorts within its own ionic volume rather than penetrates into the charge distribution of its neighbor. The opposite appears to be the case for the F^- ion.

I. INTRODUCTION

In a recent paper[1] it was demonstrated that electronic charge-overlap effects are apparent in the dynamical properties of nominally ionic crystals such as CaF_2 and SrF_2. The charge overlap is postulated to occur as a result of static or dynamic displacements of lattice ions against each other. The degree of such overlap can be expected to depend on the ability of the ions to deform under lattice displacements, i.e., on the electronic polarizabilities. In order to illuminate these points, the investigation has been repeated for $SrCl_2$ and the results are compared with those of SrF_2. In these two crystals the electronic polarizabilities[2] of the anion vary by approximately 360% (2.96 Å^3 for Cl^-, 0.644 Å^3 for F^-), whereas the electronic polarizability of the Sr^{2+} ion is essentially the same in the two lattices.

A comparison between SrF_2 and $SrCl_2$ is fortuitous on a number of other grounds. The crystal structure is the same. The ratio of the anion radius to the cation-anion nearest-neighbor distance is similar; specifically, 0.471 and 0.518,[3] respectively. Finally, the probe ion Sm^{2+}, with which the electron-lattice coupling is determined experimentally, substitutes in each case for a Sr^{2+} ion without significantly disturbing the host lattice.[4,5,6] In the paper immediately following this one a related quantity, namely the degree of static charge overlap, inherent in the formation of these crystals, is treated by Jennison and Kunz[7] in terms of a localized orbital formalism.[8] Related in turn to this calculation is the concept of ionicity. It is not immediately clear how the ionicity concept relates to the dynamical charge overlap, although it is clear that both quantities depend on the ability of the ions of the lattice to share, or transfer electronic charge, and the ability of the electronic distribution to distort as the interionic distance changes. It is accordingly, further instructive to determine if the static and dynamical electronic charge overlap show similar trends in a comparison between these lattices.

II. GENERAL EXPERIMENTAL AND THEORETICAL APPROACH

The experimental basis has been outlined in detail in Ref. 1. Only the most basic elements of the experimental background are reviewed here. The strength of the electron-phonon interaction is determined from two experimental sources. One is the vibronic sideband accompanying the electronic transition of Sm^{2+} from its ground state $4f^6(A_{1g})$ to the lowest-lying state of the $4f^55d$ excited configuration. The last named state is a very complicated one. However, since the transition is electric dipole allowed, it must terminate on the T_{1u} component of the excited state. (For further details of this state see Ref. 1.) A second experimental method is to measure the change in energy of the pure electronic transition as a function of uniaxial stress applied along a set of crystal directions. As has been shown by Kaplyanskii and Przhevuskii[9] the results lead directly to the determination of the coupling coefficients for lattice displacements transforming according to various group representations.

The general theoretical basis for the observation of vibronic sidebands and its reduction to the present case appears in Ref. 1 and in the references cited therein. The formalism leads to the following expression for the amplitude of the vibronic sidebands in terms of the imaginary part of the polarizability tensor α of the probe-ion–lattice system:

$$\mathrm{Im}\alpha_{xy}(\omega)=\frac{e^2\hbar}{4\omega}\sum_{\Gamma}\sum_{nn'}\sum_{j}F^{x}_{ab,nj}(\Gamma)\times\rho_{nn'}(\omega,\Gamma)F^{y}_{ab,n'j}(\Gamma)\,, \tag{1}$$

in which ω refers to the vibrational frequency, $\rho_{nn'}(\omega, \Gamma)$ is the density of vibrational states projected on to the nth symmetry vector belonging to the irreducible representation Γ, and $F^{i}_{ab,nj}(\Gamma)$ are components of certain coupling fields which are specified by the nature of the electronic states of the probe ion and by the electron-lattice coupling mechanism. For the particular electronic transition investigated here, $F(\Gamma)$ may be written

$$F^{i}_{ab,nj}(\Gamma) = [\langle \Psi_a(\vec{r}) | \vec{r}_i | \Psi_b(\vec{r}) \rangle / \hbar\omega] \times [\langle \Psi_a(\vec{r}) | V_{nj}(\vec{r}, \Gamma) | \Psi_a(\vec{r}) \rangle - \langle \Psi_b(\vec{r}) | V_{nj}(\vec{r}, \Gamma) | \Psi_b(\vec{r}) \rangle], \quad (2)$$

in which $\vec{r}_i$ is the ith component of the electric dipole operator, $\vec{r}$ the electron coordinate, and $V_{nj}(\vec{r}, \Gamma)$ is the symmetrized coupling field operator obtained from the coefficient of the first-order term of a Coulombic electron-lattice coupling potential expanded in terms of the displacement of the lattice ions from their equilibrium positions. It can readily be shown in terms of Eq. (2) and group-theoretic arguments that only lattice displacements transforming as A_{1g}, E_g, or T_{2g} can couple to the electronic transition described above.

Ideally, the coupling potential and the lattice displacements are obtained from microscopic models which contain realistic wave functions for the electronic distributions and which treat quantum-mechanical effects resulting from charge overlap between neighboring ions. Two approaches to such models have recently been proposed by Kühner[10] and by Wakabayaski and Sinha.[11] However, the calculations required by these methods are not currently readily reducible to the present case. The problem is, accordingly, treated in terms of a classical modified shell model described in Refs. 1 and 4. In this model charge-overlap effects on the lattice dynamics of the crystal are included through a change in the effective ionic polarizability through a reduction, from the experimental value, of the high-frequency dielectric constant. The magnitude of the change is determined using experimental data presented in Refs. 4 and 6. On the other hand, the effects of charge overlap on the interaction of the lattice with the electrons of the probe ion is treated more explicitly in terms of a further modification. This involves the replacement of the nonoverlapping electron shells of the standard shell models, with classical, extended-charge distributions which may overlap the charge distributions of neighboring ions. The actual charge distribution chosen is written

$$\rho(\vec{r}' - \vec{R}) = (1/8\pi)(Z_{\vec{R}} \lambda^3_{\vec{R}}) \exp(-\lambda_{\vec{R}} |\vec{r}' - \vec{R}|), \quad (3)$$

in which a spherically symmetric charge density ρ at the ion located in the lattice by the position vector $\vec{R}$ varies exponentially with the distance $\vec{r}'$ from that position with an exponential decay factor $\lambda_{\vec{R}}$. $Z_{\vec{R}}$ is the total shell charge of the ion ($Z_{Sr} = +10|e|$ and $Z_F = Z_{Cl} = -8|e|$ as in Refs. 1, 4, and 5). The charge distribution has a long-range behavior similar to that of a Slater ion, and resembles the electron density for the fluorine ion as obtained experimentally in CaF_2 from x-ray measurements.[12] No other justifications are offered for this form of the distribution except that it is physically reasonable and mathematically tractable. The electrons not included in the shell charge are assumed not to overlap; i.e., $\lambda = \infty$, and together with the charge of the nucleus constitute a point core charge placed at the center of the nucleus. In the calculations of the coupling strengths $V(r, \Gamma)$ and of the vibronic sideband the exponential decay factor of the anion is the only parameter to be determined.[1] All other parameters are either fixed by theory or by independent experimental data.

The relative coupling strengths of lattice displacements of the three possible symmetries (A_{1g}, E_g, T_{2g}) can now be calculated, as can the respective contributions to the vibronic sideband. As discussed in some detail in Ref. 1, the dependence of the coupling strength of a given displacement on the exponential decay factor λ_R differs, in general, from that of displacements of other symmetries. The single disposable model parameter λ, therefore, controls not only the frequency dependence of the contribution of displacement modes of a given symmetry[5] to the vibronic sideband, but also the relative contribution of modes of a given symmetry to that of modes of another symmetry.

As noted above, the ratio of the coupling strength of lattice displacements of two different symmetries can be determined independently from measurements of the effect of static stress on the localized electronic transition. The pertinent theory required to extract the coupling strengths under static strain U follows closely that for the dynamical coupling strengths V as outlined briefly above. A detailed analysis applicable to the present case appears in Refs. 9 and 13. The two coupling strengths U and V are related by a transformation proposed by Ham[14]; the applicability of which to the present case is discussed in Ref. 1.

The only disposable model parameter is accordingly chosen to agree with the results of the static stress experiment. The coupling strengths so obtained can then be used to calculate the vibronic sidebands. This is what has been done in Ref. 1 for $SrF_2:Sm^{2+}$, $SrF_2:Eu^{2+}$, $CaF_2:Sm^{2+}$, and $CaF_2:Eu^{2+}$. The agreement between experiment

and calculation is very good. The same procedure is used here for the case of $SrCl_2:Sm^{2+}$.

III. EXPERIMENTAL METHODS AND RESULTS

Standard high-resolution, low-temperature, optical-absorption spectroscopy has been used to obtain the vibronic sideband spectra.[4] The effects of uniaxial stress on pure electronic transitions in crystals held at liquid-helium temperatures can be simultaneously measured. The results for $SrCl_2:Sm^{2+}$ are reported here for the first time. In these experiments the force applied onto a fluorite crystal is measured with a Kistler model 901A quartz-crystal washer[15] which is placed immediately below the crystal. Measurements are carried out with applied stress along [100], [110], and [111] crystallographic directions. The resultant change in the absorption line can be determined using light either polarized parallel or perpendicular to the stress direction. Measurements of any resultant change in the frequency of the absorption line are determined relative to two lines of the neon spectrum superimposed onto the absorption data.

Absorption spectra have been taken for the transition in which the Sm^{2+} electronic system goes from the $4f^6(A_{1g})$ ground state to the T_{1u} component of the lowest-lying $4f^5 5d$ state. The observed Stokes sideband contains multiphonon contributions. Only the one-phonon sideband is investigated here. The experimentally obtained sideband for $SrCl_2:Sm^{2+}$ is shown in Fig. 1(a). For comparison we also show in Fig. 2(a) the corresponding sideband for $SrF_2:Sm^{2+}$ which has been previously reported in Ref. 1. In the latter case the multiphonon coupling is stronger than in the $SrCl_2:Sm^{2+}$ case and gives rise to a broad background absorption[16] sketched in by the dashed line. In these figures only the vibronic sideband is shown. The pure electronic absorption, the so-called "zero-phonon" line, has been omitted. The frequency scale refers to the lattice vibrational frequency and is obtained by measuring from the center of the zero-phonon line.

The results of the static stress measurements are given in Fig. 3 in terms of the shift in energy of the zero-phonon line as a function of applied pressure. It can be seen from Fig. 3 that, in addition to a shift in energy, the line splits when pressure is applied in the [100] and [110] direc-

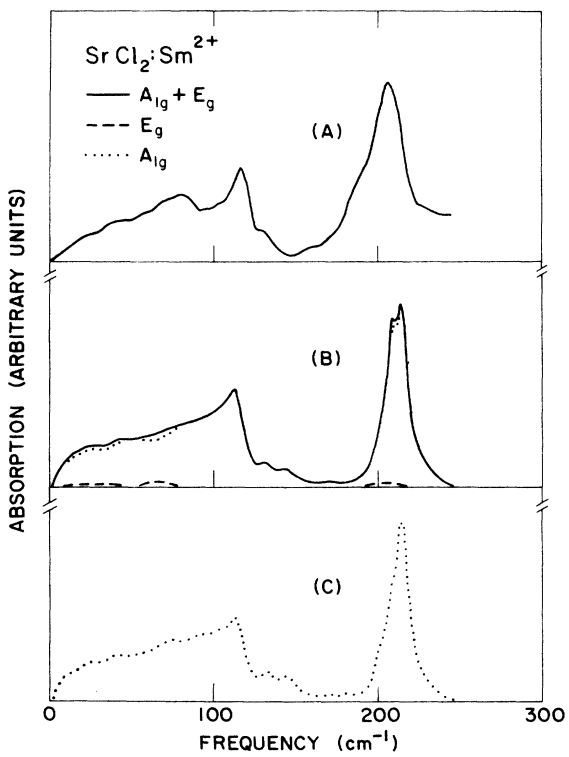

FIG. 1. Comparison between the experimentally obtained vibronic sideband in $SrCl_2:Sm^{2+}$ (a) with the calculated sideband, (b) with extended charge distributions, and (c) with nonoverlapping charges. The contribution from A_{1g} and E_g modes are separately indicated.

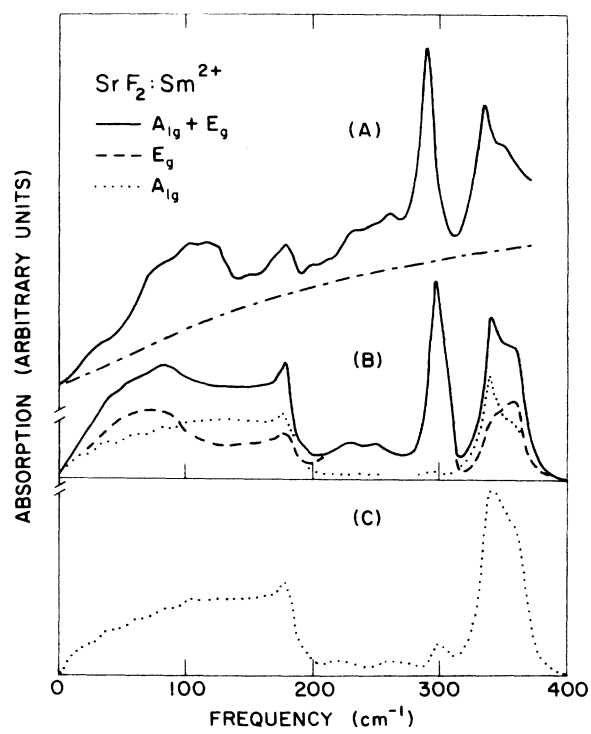

FIG. 2. Comparison between the experimentally obtained vibronic sideband in $SrF_2:Sm^{2+}$ (a) with the calculated sideband, (b) with extended charge distributions, and (c) with nonoverlapping charges. The contribution from A_{1g} and E_g modes are separately indicated. This graph has been previously published in Ref. 1.

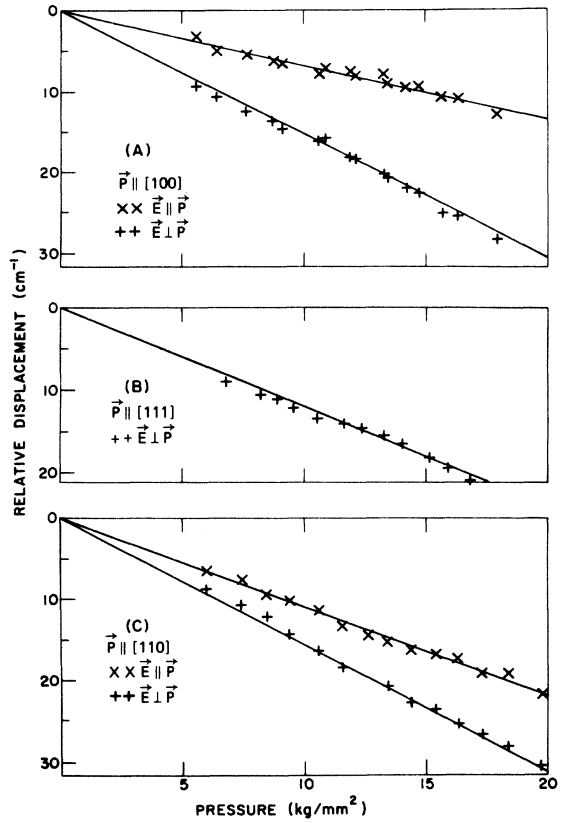

FIG. 3. Relative displacement, and splitting, of the zero-phonon line as a function of uniaxial pressure applied in the (a) [100], (b) [111], and (c) [110] crystallographic directions of $SrCl_2:Sm^{2+}$.

tions. The solid lines are least-squares fits to the data.

The static stress coefficients U' derived from the experimental data for $SrCl_2:Sm^{2+}$ are given in Table I together with those reported in Ref. 9 for $SrF_2:Sm^{2+}$. The values cited for $SrCl_2:Sm^{2+}$ are the mean of the results obtained from a series of five experiments on a number of crystals. As discussed in more detail in Ref. 1, the observation that T_{2g} displacements do not couple is a reflection of the fact that the dominant contribution to the stress dependence comes from the $5d$ electron in the excited state. The pertinent electronic state transforms as E_g in cubal symmetry and the corresponding matrix elements $\langle\Psi_b|V(\Gamma)|\Psi_b\rangle$ vanish for Γ equal to T_{2g}.

TABLE I. Stress coefficients [$cm^{-1}/(kg/mm^2)$].

	$U'(A_{1g})$	$U'(E_g)$	$U'(T_{2g})$
$SrF_2:Sm^{2+}$	-0.55[a]	0.52[a]	0[a]
$SrCl_2:Sm^{2+}$	-1.261 ± 0.077	0.319 ± 0.019	0

[a] Data from Ref. 9.

From the values of Table I and the Ham transformation[1,14] the ratio of the dynamical coupling coefficients $V(A_{1g})/V(E_g)$ can be obtained. These are 5.59 and 1.49 for $SrCl_2:Sm^{2+}$ and $SrF_2:Sm^{2+}$, respectively.

IV. COMPARISON BETWEEN EXPERIMENT AND CALCULATION

The vibronic sideband, resulting from the coupling of A_{1g} and E_g vibrational modes, is calculated through Eq. (1). (For details of the calculational methods see Ref. 1.) In the calculation the only disposable parameter is λ, i.e., the radial extent of the anion charge distribution. This parameter is varied until the ratio of the integrated sideband intensity of A_{1g} modes to that of E_g modes corresponds to the squared ratio[17] of the dynamical coupling strengths of these modes as obtained from the static stress measurements (see Sec. III). The sidebands calculated in this way for $SrCl_2:Sm^{2+}$ are shown in Fig. 1(b). For comparison the results reported in Ref. 1 for $SrF_2:Sm^{2+}$ are repeated in Fig. 2(b). For further comparison the results of calculations based on nonoverlapping (point) charges, i.e., for $\lambda \to \infty$, are shown in Figs. 1(c) and 2(c). In this case only A_{1g} modes contribute significantly to the calculated sideband.

The values for the exponential decay factors determined in this way for $SrCl_2:Sm^{2+}$ are $\lambda_{Sr} = 3.03$ Å^{-1} and $\lambda_{Cl} = 2.06$ Å^{-1}. The corresponding values for R_i', defined as the inverse of λ_i in units of the equilibrium nearest-neighbor (cation-anion) distance, are $R_{Sr}' = 0.112$ and $R_{Cl}' = 0.160$. In comparison, the corresponding values for $SrF_2:Sm^{2+}$ as stated in Ref. 1 are $\lambda_{Sr} = 1.32$ Å^{-1}, $\lambda_F = 1.13$ Å^{-1}, $R_{Sr}' = 0.30$, and $R_F' = 0.36$. The fraction of the nearest-neighbor distance at which the extended charge distribution falls to $1/e$ of its value at the origin is seen to be *smaller* in $SrCl_2$ than in SrF_2. For the case of $SrF_2:Sm^{2+}$ the ratio of the coupling strength is a strongly varying function of λ (see Ref. 1). Small changes in λ, near the value set by the results of the stress measurements, produce marked disagreement between the calculated and experimental sideband. This is not the case for $SrCl_2:Sm^{2+}$ as can be seen in the comparison of Figs. 1(b) and 1(c) for which λ_{Cl} goes from 2.06 Å^{-1} to infinity. The values cited above for λ_i and R_i' for $SrCl_2$ are, accordingly, not as well defined as the corresponding values for SrF_2. Nevertheless, the over-all good agreement between theory and experiment, demonstrated in Figs. 1(a) and 1(b), plus the very good agreement previously obtained for four separate cases,[1] suggest that the calculated values for the model parameters λ and R' for $SrCl_2$ are basically correct.

It is seen from these results, plus those of Table I, that E_g displacements couple relatively much less than A_{1g} displacements in $SrCl_2:Sm^{2+}$ compared to the relative coupling in $SrF_2:Sm^{2+}$. As shown in Ref. 1 this indicates, within the model used here, that the degree of charge overlap is *less* in $SrCl_2$ than in SrF_2. As can readily be seen from Figs. 1(c) and 2(c), in the limit of no overlap only A_{1g} modes are expected to couple.

A further interpretation of the effect of extended charge distributions has been introduced in Ref. 5 in terms of a calculated effective ionic charge. The effective charge of an ion is defined as that contained in a spherical region centered on an ion and having a radius equal to the distance of that ion from the probe ion. For the values of R_i' stated above for $SrCl_2:Sm^{2+}$, the effective ionic charges are −0.84, −1.0, +2.0 for the nearest-neighbor chlorine ions, the next-nearest-neighbor chlorine ions, and the nearest-neighbor strontium ions, respectively. The corresponding values for $SrF_2:Sm^{2+}$ are +2.6, −1.0, +2.28. The fact that in $SrF_2:Sm^{2+}$ the model parameters are such that the effective charge of the nearest-neighbor F ions is completely reversed in sign, implies that care should be exercised in assigning too much physical significance to the charge extension parameter. Nevertheless, the marked difference between $SrCl_2:Sm^{2+}$ and $SrF_2:Sm^{2+}$ in the effective charges of the nearest neighbors, together with the other evidence presented above, does support the qualitative conclusion that the degree of charge overlap caused by lattice displacements is considerably less in the case of $SrCl_2$ than in SrF_2.

V. DISCUSSION AND CONCLUSION

The result clearly shows that the degree of dynamical charge overlap is smaller in $SrCl_2$ than in SrF_2. For comparison to the parameters cited here, we have calculated, based on data from Refs. 4 and 6, the so-called dynamical effective charge[18] Z_{eff} and the Szigetti[18] charge Z^* for these lattices. These turn out to be (in units of the electron charge) $Z_{eff}=1.68$ and $Z^*=1.24$ for SrF_2, and $Z_{eff}=2.52$ and $Z^*=1.61$ for $SrCl_2$. These parameters, accordingly, also indicate that there is less dynamical charge interchange in $SrCl_2$ compared to SrF_2.

Some insight into the origin of the present results is obtained from the detailed calculations of the lattice dynamics and the electron-phonon interaction using the classical extended shell model. Displacements, from equilibrium positions, of ions with extended charge distributions toward each other, involve the possibility of charge interpenetration or charge transfer. The amount of such exchange is limited to the degree that the electronic charge distribution of one or more of the ionic species in the unit cell is polarizable. The charge distribution in a highly polarizable ion may deform within the ionic volume rather than penetrate into the space of its neighbor. The opposite phenomenon results if none of the ions is highly polarizable. According to this picture it is the high polarizability of the Cl^- ion as compared to the F^- and Sr^{2+} ion which is responsible for the lower charge overlap in $SrCl_2$ compared to SrF_2.

A quite similar conclusion can be drawn from an *a priori* calculation of the static distortions of the charge distributions and of the charge transfer in $SrCl_2$ and SrF_2 presented by Jennison and Kunz in the paper immediately following. These calculations show that the amount of charge in the overlap region is less in $SrCl_2$ than in SrF_2, and imply that the degree of electronic charge distortion is greater for the Cl^- than for the F^- ion. This trend is analogous to the trend in dynamical charge overlap reported here, but is contrary to that expected on the basis of the Pauling[19] and Phillips[20,21] ionicity scales.

What implication the present experimental results and their analysis have on the ionicity scales is not immediately apparent. The Pauling and Phillips scales are based on parameters which are, at least indirectly, also influenced by the electronic polarizabilities of the ions in the lattice. We offer only a speculation for the apparent discrepancy. The chemical bond basis for ionicity used by Pauling, and the effective band-gap basis used by Phillips, appear to be more of a measure of one-electron excitations as compared to the distortion of the electronic charge distributions as viewed by the extended charge shell model or by the localized orbital method, both of which to varying degrees treat multielectron excitations. Since distortions of the electronic distributions appear to play a major role in the effects observed here, it is possible that the latter two analytical methods yield a more consistent picture of the phenomena involved than does the ionicity concept.

ACKNOWLEDGMENTS

The authors acknowledge helpful discussions with L. L. Chase and D. H. Kühner. The authors are particularly grateful to D. R. Jennison and A. B. Kunz for making available the results of their calculation prior to publication.

*Work supported by the NSF.

†In partial fulfillment for the Ph.D. degree in physics.

[1]W. E. Bron, Phys. Rev. B 11, 3951 (1975).

[2]J. R. Tessman, A. H. Kahn, and W. Schockley, Phys. Rev. 92, 890 (1953).

[3]These ratios are determined using Pauling's ionic radii and standard values for the nearest-neighbor distance.

[4]D. H. Kühner, H. V. Lauer, and W. E. Bron, Phys. Rev. B 5, 4112 (1972).

[5]L. L. Chase, D. H. Kühner, and W. E. Bron, Phys. Rev. B 7, 3892 (1973).

[6]D. H. Kühner and M. Wagner, Z. Phys. 256, 22 (1972).

[7]D. R. Jennison and A. B. Kunz, following paper, Phys. Rev. B 13, 5597 (1976).

[8]A. B. Kunz, Phys. Status Solidi 36, 301 (1969); Phys. Rev. B 2, 2224 (1970); 4, 603 (1971).

[9]A. A. Kaplyanskii and A. K. Przhevuskii, Opt. Spectrosk. 20, 557 (1966).

[10]D. H. Kühner, Phys. Rev. B 9, 1792 (1974).

[11]N. Wakabayaski and S. K. Sinha, Phys. Rev. B 10, 745 (1974); see also S. K. Sinha, R. P. Grypta, and D. L. Price, Phys. Rev. B 9, 2564 (1974); 9, 2573 (1975).

[12]H. Witte and E. Wölfel, Rev. Mod. Phys. 30, 51 (1958).

[13]A. A. Kaplyanskii, Opt. Spectrosk. 16, 557 (1964).

[14]F. S. Ham, Phys. Rev. 166, 307 (1968).

[15]Kistler Instrument Corp., Clarence, N.Y.

[16]W. E. Bron and M. Wagner, Phys. Rev. 139, A233 (1965).

[17]The square of the ratios is required because the product of the force fields F appears in Eq. (1).

[18]See, e.g., E. Burstein, in *Phonon and Phonon Interactions*, edited by T. A. Bak (Benjamin, New York, 1964); see also S. K. Sinha, CRG Crit. Rev. Solid State Sci. 3, 273 (1973).

[19]L. Pauling, *The Nature of the Chemical Bond*, 3rd ed. (Cornell University, Ithaca, 1960).

[20]J. C. Phillips, Rev. Mod. Phys. 42, 317 (1970); see also J. C. Phillips, Phys. Rev. Lett. 20, 550 (1968); and J. A. Van Vechten, Phys. Rev. 182, 891 (1969); 187, 1007 (1969).

[21]B. F. Levine, J. Chem. Phys. 59, 1463 (1973).